

Comparing Machine Learning Algorithms for Surface Water Mapping using Sentinel-1 Data

Xanthoula-Eirini Pantazi¹, Ines Cherif², Afroditi-Alexandra Tamouridou¹,
Dimitrios Moshou¹, Georgios Ovakoglou², Thomas Alexandridis², Xanthi Tseni³,
Stella Kalaitzopoulou³ and Spiros Mourelatos³

¹Laboratory of Agricultural Engineering, School of Agriculture, Aristotle University of Thessaloniki, Thessaloniki 54124, Greece; e-mail: dmoshou@agro.auth.gr

²Laboratory of Remote Sensing, Spectroscopy and GIS, School of Agriculture, Aristotle University of Thessaloniki, Thessaloniki 54124, Greece; e-mail: thalex@agro.auth.gr

³Ecodevelopment S.A., Fyliro 57010, Thessaloniki, Greece; e-mail: info@ecodev.gr

Abstract. Determining the presence and extent of surface water bodies is of paramount importance in order to monitor mosquito breeding habitats. With the availability of high spatial and temporal resolution SAR images through the Sentinel-1 mission, it becomes possible to map surface water on a regular basis in mosquitos' prone areas. In this work the potential of Machine Learning (ML) algorithms is investigated for the near-real time mapping of surface water in the Chalastra plain in Central Macedonia in Greece, using Sentinel-1 data. Three ML algorithms: One-Class SVM, One-Class Self-Organizing Map, and Multilayer Perceptron with Automatic Relevance Determination (MLP-ARD) were compared to the Otsu Valley-Emphasis method, a commonly used approach based on histogram thresholding. All methods were automated and tested in the pilot area. Results show that the MLP-ARD algorithm achieves the highest overall accuracy (0.974) among all methods with a kappa coefficient of 0.933.

Keywords: inundated area; remote sensing; SAR; one-class classifier; MLP-ARD.

1 Introduction

The distribution of surface water bodies varies with time and space depending on weather conditions, irrigation patterns, as well as different water uses. Regular mapping of water bodies is a good practice towards the sustainable management of water resources. Water ponds, wetlands, inundated rice, and flooded areas are some major habitats of mosquitoes' breeding. Monitoring the presence of water helps identifying hotspots of mosquitoes' larvae development, for targeted and effective larvicide application, in order to reduce their potential harm to human health. With a rational use of such larvicides the impact on water resources will be minimized.

Copyright © 2020 for this paper by its authors. Use permitted under Creative Commons License Attribution 4.0 International (CC BY 4.0).

Proceedings of the 9th International Conference on Information and Communication Technologies in Agriculture, Food & Environment (HAICTA 2020), Thessaloniki, Greece, September 24-27, 2020.

Remote sensing data, both radar and optical, were widely used for monitoring surface water from space. Optical satellite data were used to produce surface water indicators (e.g. the Normalized Difference Vegetation Index - NDVI, the Normalized Difference Water Index - NDWI and the Modified NDWI - MNDWI) (Xu 2006, Xiao, et al. 2002, Du, et al. 2016) but their performance is limited to clear-sky conditions. Radar data have the advantage of providing information even under cloudy conditions thus are more appropriate for monitoring activities (Martinis, et al. 2015, Duy 2015, Betbeder, et al. 2014, Li and Wang 2015), but terrain effects introduce errors in water detection (Huang, et al. 2017).

There is also an emerging trend in the literature (Komarkova, et al. 2019, Imam, et al. 2020) that is using images from drones to achieve higher spatial and temporal resolution. However, these have very limited coverage as compared to satellites and are not fit for wide areas at the regional or national scale level. With the European Union's Copernicus Programme, Sentinel-1 data became available every 6 days with a high spatial resolution (10 m), making the use of Synthetic Aperture Radar (SAR) data convenient for mapping water bodies' extent over a long time period, independently of cloud cover.

In order to identify pixels with water on satellite images, histogram thresholding was widely used with multispectral and SAR data (Duy 2015, Martinis, et al. 2009, Bioresita, et al. 2018, Bangira, et al. 2019). The Otsu method (Otsu 1975) is the most popular method for threshold identification, some revised approaches were then proposed such as the Valley Emphasis thresholding method (Ng 2006).

ML combined with remote sensing techniques have been utilized widely in order to detect temporal and spatial alterations in small waterbodies so as to provide information in the field of water security, drought monitoring, and crop irrigation decision-making. The above combination forms a reliable, cost-effective, solution for surface water mapping in large and inaccessible areas. Bangira et al. (2019), proposed a such an approach based on the effective combination of automatic thresholding of NDWI using Sentinel-2 and backscatter from Sentinel-1 data with VH polarisation for mapping waterbodies of diverse spectral and spatial characteristics. The resulting maps were compared to the classification performances of five ML algorithms, namely decision tree (DT), k-nearest neighbor (k-NN), random forests (RF), and two implementations of the support vector machine (SVM), enhancing the accurate classification of optically complex waterbodies.

In the present work three ML algorithms are presented and tested against a classical method of histogram thresholding for the automatic mapping of surface water bodies in the Chalastra plain, Greece.

2 Study area and field data

The study area is the plain of Chalastra, which is the lowest part of the floodplain of rivers Axios and Loudias (Greece). It is intensely cultivated with irrigated annual crops, most predominantly with paddy rice. Numerous drainage canals, river segments, and their estuaries have formed a complex wetland system (Fig. 1).

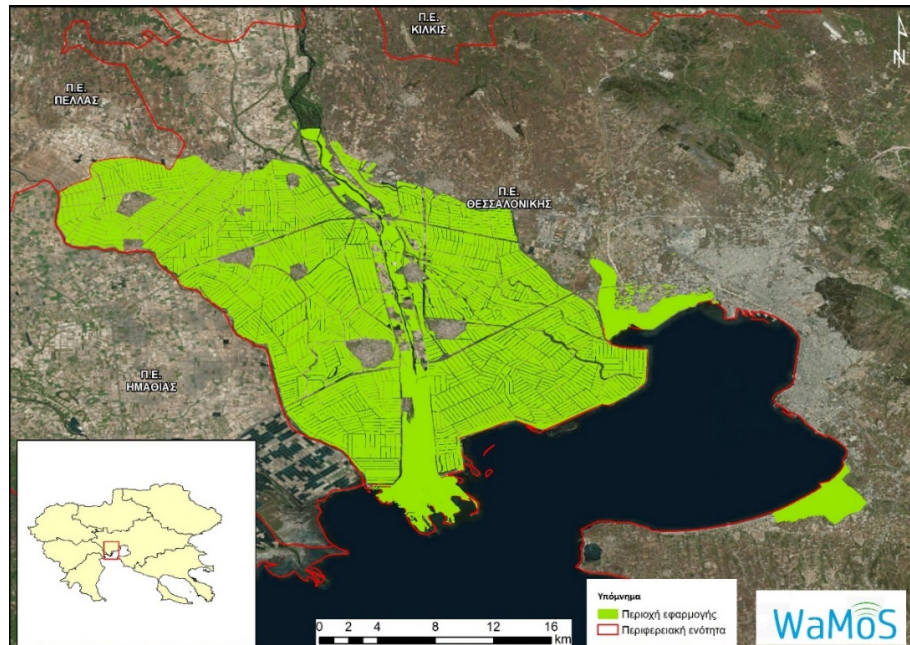


Fig. 1. Study area where the measurements have been taken.

A field campaign was conducted during summer 2019 to collect ground data of wet and dry polygons in the wider area around Chalastra. The samples were taken at dates concurrent with the overpass of Sentinel-1. Sampling locations consisted in rice fields (inundated during the early season and presenting different plant growth stages) and wetlands which are typical breeding habitats but also built areas, natural vegetation and dry soils which can challenge the water detection algorithms and help training the ML ones. The mapped polygons were characterized by different water depths and vegetation cover. On the date of June 12th 2019, a total of 30 polygons were collected

leading to a total of 16866 10-by-10m pixels labelled as wet or dry in the test area.

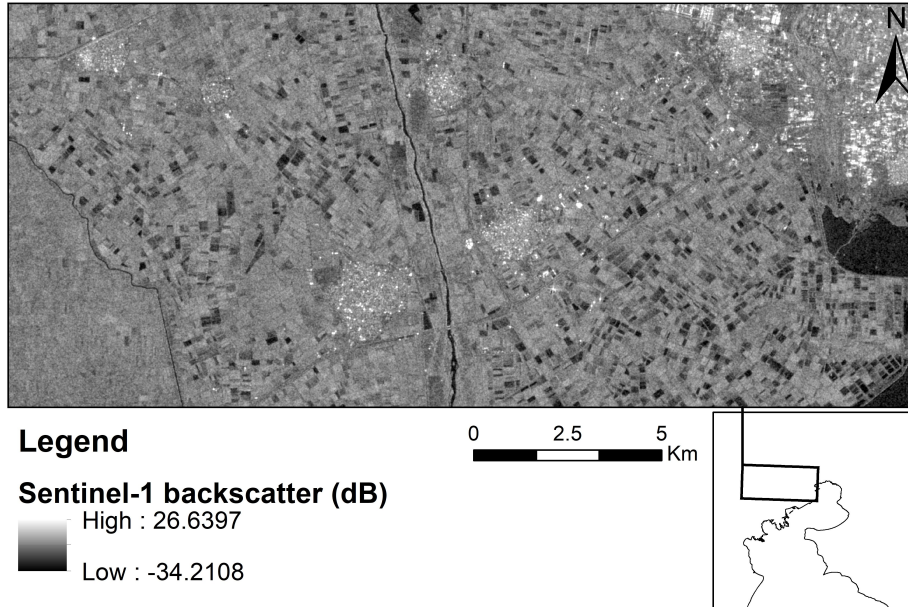


Fig. 2. Sentinel-1 backscatter map with VV polarization for the pilot area on 12/6/2019.

3 Methods

A Sentinel-1 image was downloaded using Google Earth Engine (GEE) with both VV and VH polarizations, Ground Range Detected (GRD) type and in Interferometric Wide swath (IW) mode. The downloaded image was already pre-processed in GEE as proposed by the Sentinel-1 Toolbox and saved as Geotiff data file with the backscatter given in decibel. A section of the image was used for processing (2552*1102 pixels) (see Fig1).

Four surface water mapping algorithms were implemented in Matlab and tested on the Sentinel-1 image of June 12th, 2019. In particular, three ML algorithms were compared to a revised histogram thresholding method.

3.1 One Class SVM (OC-SVM)

To achieve One Class SVM Classification, a suitable description of SVM as a model to describe only target data introduced by Tax and Duin (2004) in the form of Support Vector Data Description (SVDD) has been applied. The OC-SVM develops a model by being trained in using normal data conforming to the SVDD description. At the second stage, it allocates test data based on the occurring deviation from normal calibration data as being either normal or outlier (Scholkopf, 2002).

$$K(\mathbf{x}, \mathbf{z}) = \exp\{-\|\mathbf{x} - \mathbf{z}\|^2 / \sigma^2\} \quad (1)$$

It can be determined by considering that a sizeable spread indicates a linear class of target data while on the other hand, many support vectors joint with a small spread indicate a highly nonlinear case as is illustrated in Figure 2. A spread parameter equivalent to 1 yielded the best results concerning waterbodies detection. The threshold for accepting outliers was set at 10 %.

3.2 One Class Self-Organizing Map (OC-SOM)

The OC-SOM constructs a model from target data (dry areas) and progressively classifies new data conferring to its deviation from the target baseline condition. During novelty recognition, novel instances from feature combinations (in the current case the features from the S1 image) of not definable state validation data samples, are used to form the input to the network, while the SOM algorithm chooses the Best Matching Unit (BMU). In the current application, the BMU is defined as the most proximal SOM centroid vector in the weights space to the incoming data vector. In the occasion that the quantisation error that is the outcome from the appraisal between the new exemplar data (x^{NEW}) and BMU is larger than a pre-specified threshold (d) then the example is considered as novel (Saunders & Gero, 2001).

3.3 Multilayer Perceptron with Automatic Relevance Determination (MLP-ARD)

MLPs are feed forward artificial neural networks, that in classification problems map a set of input vectors onto their respective classes. For this study, a fully connected MLP with a three – layer architecture (input layer, hidden layer and output layer) is assigned for the classification of the spectral signatures into the healthy or the intensity of the disease level conditions. The weights correction is performed by the scaled conjugate gradient back propagation algorithm and the transfer function that were selected were the hyperbolic tangent (tanh) for the interconnections between the input and the hidden layer and the logistic function for the respective interconnections between the hidden and the output layer.

Apart from the first level hyperparameters, the values of which are randomly chosen as priors for the initialization of the MLP classifiers, Automatic Relevance Determination (ARD) is used in this study. In the application of the ARD technique a new regularization hyperparameter, alpha (α) is introduced, for every weight that is associated to the i input variables, in order to determine the relevance of the input data into the model (Pantazi et al., 2017).

3.4 Otsu Valley-Emphasis (OVE)

The Otsu Valley-Emphasis method (Ng 2006) is an improved Otsu algorithm for finding automatically a threshold in the SAR backscatter histogram (Otsu 1975). The method maximizes the inter-class variance and minimizes the weighted within-class variance, while giving weight to the valley points in the histogram in order to favor values that reside at the valley of two peaks or at the bottom rim of a single peak. Only VV-polarized Sentinel-1 data were used as input to the OVE method (Twele et al., 2016).

4 Results

For the implementation and assessment of the ML algorithms the field survey dataset was split. 11806 samples were used for training and 5060 for validation, while the Otsu Valley-Emphasis method was validated using the whole dataset. All four methods were implemented using Matlab version R2019b.

The results of the best performing ML algorithm the MLP-ARD are presented in Figure 3.

Table 1. Confusion matrix results for the four methods tested.

Algorithm	Precision	Recall	Overall accuracy	Kappa
OC-SOM	0.917	0.977	0.925	0.820
OC-SVM	0.895	0.986	0.915	0.802
MLP-ARD	0.987	0.977	0.974	0.933
OVE	0.906	0.903	0.948	0.869

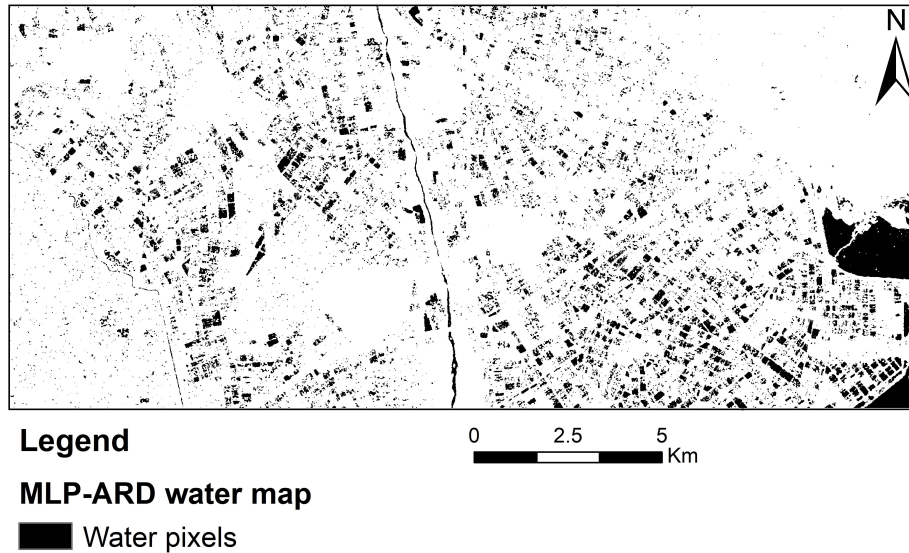


Fig. 3. Surface water map of the pilot area on 12/6/2019 using the MLP-ARD algorithm.

The MLP-ARD method led to the highest overall accuracy of 0.974 with a kappa coefficient of 0.933. The precision and recall metrics for this method are respectively 0.987 and 0.977, higher than for the other methods meaning that false alarms and missed detections are minimized.

The other two one-class ML methods OC-SVM and OC-SOM provided a lower accuracy than the Otsu Valley-Emphasis method. However, in precision and recall OC-SOM algorithm supersedes OVE. Both OC algorithms have equal or better recall than the OVE. This result can be explained by the OC algorithms 'excellent outlier detection capability with the recall of OC-SVM reaching a performance of 0.986.

As shown in Fig 3, the sea, riverbed and coastal wetlands were detected by the MLP-ARD algorithm with few missed detections. Unlike for the one-class algorithms, the built areas in the neighboring villages did not cause false alarms.

The computation time required to train the OC and MLP -ARD algorithms is minimal and requires very few minutes. For producing a prediction map for waterbodies detection with a size of over 2.8 M pixels, different time was required for the two OC algorithms (few hours), which appeared to be a limiting factor for near-real time application. Both the MLP-ARD and OVE methods produced maps in a reasonable time (few minutes).

5 Conclusion

Both the Otsu Valley-Emphasis and MLP-ARD algorithms provided good accuracy for the detection of water bodies using high-resolution SAR images. Due to the generalization capability of the MLP-ARD, the trained network can be applied further without any retraining and can generalize over new example images acquired from different days and years. A more robust version of the MLP-ARD will be produced by training by data from different days' time series of Sentinel-1 images will be processed using the MLP-ARD to monitor surface water bodies during the whole summer season of 2019. Results will be presented in a future communication.

Acknowledgments. This research has been co-financed by the European Regional Development Fund of the European Union and Greek national funds through the Operational Program Competitiveness, Entrepreneurship and Innovation, under the call RESEARCH – CREATE – INNOVATE (project code: T1EDK-05106).

References

1. Xu, H. 2006 Modification of normalised difference water index (NDWI) to enhance open water features in remotely sensed imagery. *International Journal of Remote Sensing*, 27 (14), 3025-3033.
2. Xiao, X., Boles, S., Frohling, S., Salas, W., Moore, B., Li, C. et al. 2002 Observation of flooding and rice transplanting of paddy rice fields at the site to landscape scales in China using VEGETATION sensor data. *International Journal of Remote Sensing*, 23 (15), 3009-3022.
3. Du, Y., Zhang, Y., Ling, F., Wang, Q., Li, W. and Li, X. 2016 Water Bodies' Mapping from Sentinel-2 Imagery with Modified Normalized Difference Water Index at 10-m Spatial Resolution Produced by Sharpening the SWIR Band. *Remote Sensing*, 8 (4), 354.
4. Martinis, S., Kersten, J. and Twele, A. 2015 A fully automated TerraSAR-X based flood service. *ISPRS Journal of Photogrammetry and Remote Sensing*, 104, 203-212.
5. Duy, N.B. 2015 Automatic detection of surface water bodies from Sentinel-1 SAR images using Valley-Emphasis method. *Vietnam Journal of Earth Sciences*, 37 (4), 328-343.
6. Betbeder, J., Rapinel, S., Corpetti, T., Pottier, E., Corgne, S. and Hubert-Moy, L. 2014 Multitemporal classification of TerraSAR-X data for wetland vegetation mapping. *Journal of applied remote sensing*, 8 (1), 083648.
7. Li, J. and Wang, S. 2015 An automatic method for mapping inland surface waterbodies with Radarsat-2 imagery. *International Journal of Remote Sensing*, 36 (5), 1367-1384.

8. Huang, C., Nguyen, B.D., Zhang, S., Cao, S. and Wagner, W. 2017 A Comparison of Terrain Indices toward Their Ability in Assisting Surface Water Mapping from Sentinel-1 Data. *ISPRS International Journal of Geo-Information*, 6 (5), 140.
9. Martinis, S., Twele, A. and Voigt, S. 2009 Towards operational near real-time flood detection using a split-based automatic thresholding procedure on high resolution TerraSAR-X data. *Natural Hazards and Earth System Sciences*, 9 (2), 303-314.
10. Bioresita, F., Puissant, A., Stumpf, A. and Malet, J.-P. 2018 A Method for Automatic and Rapid Mapping of Water Surfaces from Sentinel-1 Imagery. *Remote Sensing*, 10 (2).
11. Bangira, T., Alfieri, S.M., Menenti, M. and van Niekerk, A. 2019 Comparing Thresholding with Machine Learning Classifiers for Mapping Complex Water. *Remote Sensing*, 11 (11), 1351.
12. Tax, D. M., & Duin, R. P. 2004. Support vector data description. *Machine learning*, 54(1), 45-66.
13. Scholkopf, B.; Smola, A.J. *Learning with Kernels: Support Vector Machines, Regularization, Optimization, and Beyond*; MIT Press: Cambridge, MA, USA, 2002.
14. Saunders, R., & Gero, J. S. 2001. A curious design agent: A computational model of novelty-seeking behaviour in design.
15. Pantazi, X. E., Moshou, D., Oberti, R., West, J., Mouazen, A. M., & Bochtis, D. 2017. Detection of biotic and abiotic stresses in crops by using hierarchical self organizing classifiers. *Precision Agriculture*, 18(3), 383–393.
16. Otsu, N. 1975 A threshold selection method from gray-level histograms. *Automatica*, 11, 23-27.
17. Ng, H.-F. 2006 Automatic thresholding for defect detection. *Pattern Recognition Letters*, 27 (14), 1644-1649.
18. Twele, A., Cao, W., Plank, S. and Martinis, S. 2016 Sentinel-1-based flood mapping: a fully automated processing chain. *International Journal of Remote Sensing*, 37 (13), 2990-3004.
19. Komarkova, J., Cermakova, I., Sedlak, P. and Jech, J. 2019 Spectral Enhancement of Imagery for Small Inland Water Bodies Monitoring: Utilization of UAV-Based Data. *Journal of Information Systems Engineering and Management*, 4 (4), em0102.
20. Imam, R., Pini, M., Marucco, G., Dominici, F. and DAVIS, F. 2020 UAV-Based GNSS-R for Water Detection as a Support to Flood Monitoring Operations: A Feasibility Study. *Applied Sciences*, 10 (1), 210.